Alex. Eng. J., Alex. Univ., Volum, 28 No. 2, PP. 61 - 78 (1989)

VIBRATIONS OF THIN ISOTROPIC TRUNCATED CONICAL SHELLS WITH GEOMETRIC IMPERFECTIONS

S.F. Rezeka and A.A. Helmy

Assistant Professor Assistant Professor

Department of Mechanical Engineering

Alexandria University, Egypt

Abstract

The effect of initial geometric imperfections on large amplitude vibrations of a truncated conical shell subjected to pressure load has been investigated. The analysis of the problem is based on the solution of Donnell-type dynamic equations and compatibility equation for conical shells in terms of stress function and an out-of-plane displacement. The geometric imperfections are taken to be of the same spatial shape as the vibration mode. Based on the assumed sinusoidal vibration mode shape, the stress function that satisfies the nonlinear compatibility equation is exactly sought. The nonlinear dynamic equation is then satisfied approximately using the Galerkin procedure. The influence of shape factor, meridional and circumferential wave number, and in-plane boundary conditions on the vibration frequency has been discussed. It was found that the presence of geometric imperfection softens the shell behavior and the softening increases with the apex rise.

Nomenclature

D	Flexural rigidity.
E	Young modulus of elasticity.
F,f	Stress function, dimensionless stress function.
h	Shell thickness.
$\sqrt{k}$	Linear vibration frequency.
L,L_o	Shell lengthes (Figure 1)
m	Meridional wave number.
n	Circumferential wave number.
$N_s,N_\theta,N_{s\theta}$	Stress resultant.
p	Pressure.
$\bar{t}$, t	Time, dimensionless time.
u,v,w	Dimensionless displacement.
X	Vibration amplitude.
Z	Shape factor.
β	Cone angle.
γ	L/L_o
μ	Imperfection amplitude.
ν	Poisson's ratio.
ω_r	Reference frequency.
Ω	Dimensionless frequency.

Introduction

The truncated conical shell has received great attention in recent years because its wide applications in aerospace and mechanical engineering. Esslinger and Geier [1]studied buckling and postbuckling behavior of conical shells subjected to axisymmetric loading and

discussed the design criteria for thin-walled shells. Hubner [2] investigated large deformations of axisymmetric elastic conical shells under axial forces on the basis of Reissner-Meissner equation. The practical design of conical springs and the criterion of stability were considered. Tani [3] obtained the static response of clamped truncated conical shells under two loads combined out of uniform pressure, axial load and uniform heating, taking into consideration the effect of nonlinear prebuckling deformation.

As for the dynamic behavior, Massalas et al. [4] examined the free vibration, the classical buckling, and the dynamic instability of a clamped truncated conical shell with variable modulus of elasticity and subjected to periodic axial compressive force. They solved Donnell's equation for membranes by applying the Galerkin method and Bolotin's procedures. Dumir and Khatri [5] used the orthogonal point collocation method and Newmark-β scheme to investigate the static and dynamic buckling of orthotropic truncated conical caps. Dumir [6] presented an approximate analytical solution of the large deflection axisymmetric response of the polar orthotropic thin truncated shallow shells.

The effects of geometric imperfections on large amplitude vibrations of rectangular plates, circular plates, spherical shells, cylindrical panels, and oval panels were examined by Hui et al. [7,8,9,10,11]. Watawala and Nash [12] investigated the effects of imperfection on nonlinear vibration of closed cylindrical shells.

It appears from the previous review that the effects of geometric imperfections on large-amplitude vibrations of thin truncated conical shells have not been examined and this is the purpose of this work. In the analysis the effect of in-plane boundary conditions, shape factors, and mode number are also investigated.

Mathematical Formulation

The configuration of truncated conical shell subjected to pressure p, and the coordinate system are shown in Figure 1. The displacement components along the middle surface are denoted by U, V, and W. F is considered as the stress function and is related to the stress resultant as:

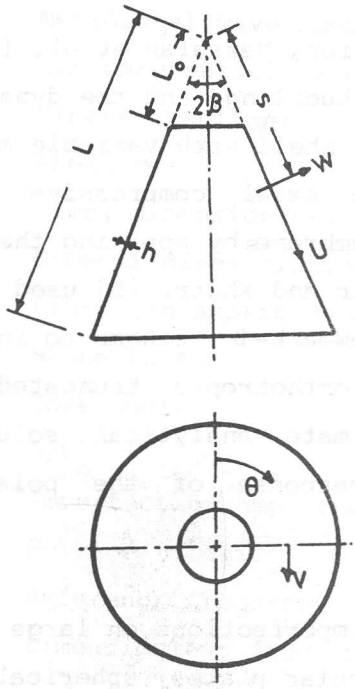

Figure 1: Geometry of a conical shell and coordinate system.

$$N_\theta = F_{,ss}$$

$$N_s = -\frac{1}{s} F_{,s} + \frac{1}{s^2 \sin^2 \beta} F_{,\theta\theta} \qquad (1)$$

$$N_{s\theta} = -\left(\frac{1}{s \sin \beta} F_{,\theta} \right)_{,s}$$

The dynamic analogue of the nonlinear Donnel-type differential equation, and the compatibility equation for isotropic conical shells written in terms of the out-of-plane displacement and the stress function, incorporating the presence of geometric imperfection w_o, are given in nondimensional form as follows:

$$\nabla^4 w = e^{3y}(f_{,yy} + f_{,y})Z + e^{4y}\,[f_{,\varphi\varphi} - f_{,y}][(w+w_o)_{,yy} + (w+w_o)_{,y}]$$

$$+ e^{4y}\,[f_{,yy} + f_{,y}][(w+w_o)_{,\varphi\varphi} - (w+w_o)_{,y}]$$

$$- 2e^{4y}\,[f_{,\dot{\varphi}} + f_{,\dot{\varphi}y}][(w+w_o)_{,\varphi} + (w+w_o)_{,y\varphi}]$$

$$+ Zk_p - Z\,w_{,tt} \qquad (2)$$

$$\nabla^4 f = -12\,Ze^{3y}\,[w_{,yy} + w_{,y}] + 12e^{4y}\,[w_{,y}[(w+w_o)_{,yy} + (w+w_o)_{,y}]$$

$$+ w_{o,y}\,(w_{,yy} + w_{,y}) - (w+w_o)_{,\varphi\varphi}\,(w_{,yy} + w_{,y})$$

$$- w_{,\varphi\varphi}\,(w_{o,yy} + w_{o,y}) + w^2_{,y\varphi} + 2w_{,y\varphi}w_{o,y\varphi} + w^2_{,\varphi}$$

$$+ 2w_{,\varphi}\,w_{o,\varphi} + 2w_{,\varphi}(w+w_o)_{,y\varphi} + 2\,w_{o,\varphi}\,w_{,y\dot{\varphi}}] \qquad (3)$$

where

$$y = \ln\frac{L}{s}\,,\quad \varphi = \theta\sin\beta\,,\quad (u,v) = \frac{\sqrt{1-\nu^2}}{h\cot\beta}(U,V),$$

$$w = \sqrt{1-\nu^2}\,\frac{W}{h}\,,\quad f = \frac{F}{D}\,,\quad Z = \frac{\sqrt{1-\nu^2}\,L}{h\tan\beta}$$

$$D = \frac{Eh^3}{12(1-\nu^2)}\,,\quad k_p = \frac{pL^3\tan\beta}{D}\,,\quad t = \omega_r\bar{t}\,,$$

$$\omega_r^2 = \frac{Eh}{12\rho L^3\tan\beta}\,,\qquad \gamma = \frac{L}{L_o}$$

ν is Poisson's ratio, E is Young's modulus, ρ is the density, D is the flexural rigidity, $\bar{t}$ is the time, Z is the shape factor, and ω_r is the reference frequency.

It should be noted that in case of static perfect conical shell ($w_o = 0$, and $w_{,tt} = 0$), equations 2 and 3 are reduced to the equations developed by Tani (1985). The geometric imperfection w_o appears only in the terms that describe the difference in shape between the deformed element and an element of a perfect cone. These terms are not traced back to the elastic law.

The in-plane displacement components are related to f and w by:

$$N^*_s - \nu N^*_\varphi = e^y (f_{,\varphi\varphi} - f_{,y}) - \nu (e^y f_{,y})_{,y}$$

$$= 6 e^y W_{,y} (w+2w_o)_{,y} - 12 Z u_{,y} \qquad (4\text{-a})$$

$$N^*_\varphi - N^*_s = 12 Z (v_{,\varphi} + u + w) + 6e^y w_{,\varphi} (w+2w_o)_{,\varphi} \qquad (4\text{-b})$$

In the analysis it is assumed that the conical shell is clamped at both ends : i.e ;

$$w = w_{,y} = 0 \qquad \text{at} \qquad y = 0,\ y = \ln\gamma \qquad (5\text{-a})$$

Three in-plane boundary conditions are considered:

I. There are a tangential constraints and no meridional constraints at both ends

$$\text{i.e} \qquad N_s = 0 \quad , \quad v = 0 \qquad (5\text{-b-I})$$

II. There are meridional constraints and no tangential constraints at both ends

$$\text{i.e} \quad N_{\varphi} = 0 \ , \quad u = 0 \qquad \text{(5-b-II)}$$

III. There are meridional and tangential constraints at both ends (fixed ends)

$$\text{i.e} \quad u = v = 0 \qquad \text{(5-b-III)}$$

Method of Solution

The vibration mode, the initial geometric imperfection, and the forcing function are assumed to have the same spatial distribution such that

$$[w(y,\varphi,t),\ w_o(y,\varphi),\ k_p(y,\varphi,t)] = [w(t),\mu,\ k_p(t)](\cos n\varphi)$$

$$\left[\cos \frac{(m-1)\pi}{\ln \gamma} y - \cos (m+1)\pi\right] n \qquad (6)$$

where $w(t)$, and μ are the normalized vibration and imperfection amplitudes, m and n are the number of meridional and circumferential waves respectively.

It should be mentioned that an arbitrarily specified shape of the geometric imperfection can be expanded in terms of a Fourier series in the meridional and circumferential directions.

Substituting $w_o(y, \varphi)$ and $w(y, \varphi, t)$ into equation (3), yields the stress function that satisfies the nonlinear compatibility equation

$$f(y, \varphi, t) = A_o\, w(t)\, e^{-y} [\, M \cos n\varphi \cos My + \cos n\varphi \sin My \,]$$
$$+ [w^2(t) + 2\mu\, w(t)][A_1(y^2 + \varphi^2) + A_2 \cos 2My + A_3 \cos 2n\varphi$$
$$+ A_4 \sin 2My + A_5 \sin My + A_6 \cos My + A_7 \cos 2My \cos 2n\varphi$$
$$+ A_8 \sin 2My \cos 2n\varphi + A_9 \cos My \cos 2n\varphi$$
$$+ A_{10} \sin My \cos 2n\varphi + E_1 y + E_2 \varphi^2/2] \qquad (7)$$

where $M = (m-1)\,\pi / \ln\gamma$

$A_o, \ldots, A_{10}$ are functions of M and n (Appendix)

E_1, and E_2 are depending on the in-plane boundary conditions (Appendix)

Substituting $w(y, \varphi, t)$, $w_o(y, \varphi)$, and $f(y, \varphi, t)$ into the nonlinear equilibrium equation and applying the Galerkin procedure, one obtains the equation of motion in terms of w(t)

$$w(t)_{,tt} + [\, k\, w(t) + (\varepsilon k a_2) w^2(t) + (\varepsilon k) w^3(t)] = k_p(t) \qquad (8)$$

Equation (8) is the Duffing-type differential equation with an additional quadratic term. The linear free vibration frequency is

$$\Omega_o = \sqrt{k} \qquad (9)$$

Assuming that the forcing function is $k_p = k_{p1} \cos \Omega t$, the solution of the linearized differential equation is

$$w(t) = X \cos \Omega t \qquad (10)$$

and $|X| = (k_{p1}/k)/(1 - \Omega^2/k)$

The backbone curves for large amplitude free vibrations of imperfect truncated conical shell can be computed by solving the Duffing-type equation using Linstedt's perturbation method. It follows that the ratio of the nonlinear to the linear vibration frequency Ω / Ω_o is related to the vibration amplitude X and the nonlinearity parameter r by (Hui, 1983):

$$\Omega / \Omega_o = 1 + r X^2 - (15 \varepsilon^2 X^4/256)$$

and (11)

$$r = (3 \varepsilon/8) - (5a_2^2 \varepsilon^2/12)$$

Thus, at least for sufficient small values of the vibration amplitude X, the nonlinear hard-spring or soft-spring behavior is indicated respectively, by positive or negative values of the non-linearity parameter r (the behavior tends to be more pronounced for large magnitude of r).

Results and Discussions

The following results are obtained for a conical shell with cone angle $\beta = 30^o$. The influence of the initial geometric imperfection μ on the linear vibration frequency $\sqrt{k}$ for various values of Z and γ is illustrated in Figure 2 for m = 3 and n = 2, and in Figure 3 for m = 5 and n = 2. The results are independent of the sign of the geometric imperfection. Therefore, the plots are for positive values of μ only. It can be noticed from both Figures 2 and 3 that the linear-vibration frequency for the perfect conical shell ($\mu = 0$) does not depend on the type of in-plane boundary conditions. For a fixed value of μ, the linear frequency increases with the increase of the shape factor Z. Keeping the value of Z constant, the presence of the geometric imperfection increases the linear vibration frequency for γ =2 for all different considered in-plane boundary conditions. For $\gamma = 6$, m = 5

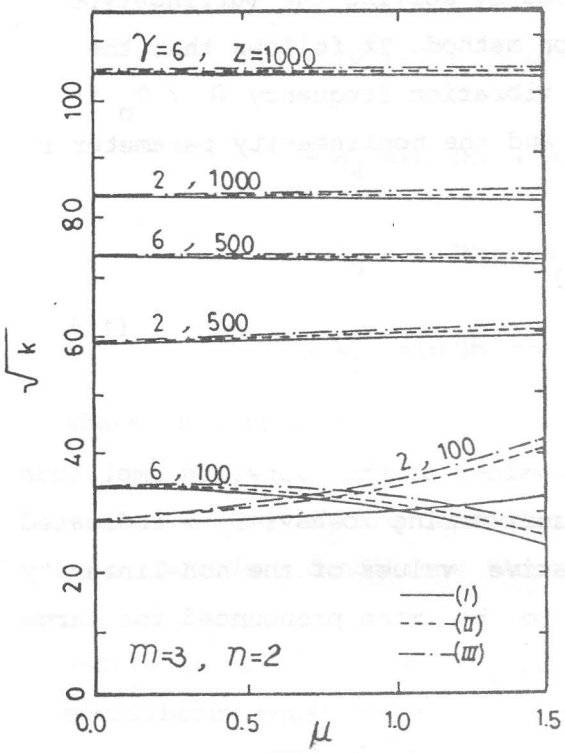

Figure 2: Linear frequency versus imperfection amplitude for m = 3, n = 2, Z = 100, 500, 1000, and γ = 2,6.

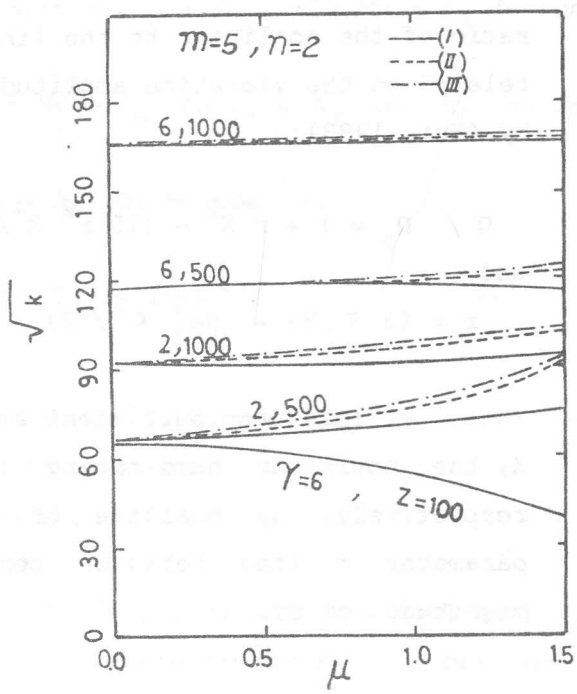

Figure 3: Linear frequency versus imperfection amplitude for m = 5, n = 2, Z = 100, 500, 1000, and γ = 2,6.

and n = 2, as the geometric imperfection amplitude increases, the associated linear vibration frequency increases except when the meridional constraints are released (case I). In this case, increasing the value of lowers the vibration frequency. However, for γ =6, m = 3 and n = 2, increasing the amplitude of the imperfection results in a reduction in the linear frequency regardless of the type of in-plane boundary conditions. It is clear from Figures 2 and 3 that the effect of geometric imperfection on linear-vibration frequency decreases considerably as Z increases.

The nonlinearity parameter r, resulted upon imposing an imperfection μ , is presented in Figures 4,5, and 6. It appears from the figures that, for γ =2, small amplitudes of geometric imperfection result in hard-spring behavior (positive r). But as the imperfection amplitude increases it tends to soften the shell. For γ = 6, the presence of geometric imperfection softens the shell and the softening becomes more pronounced as μ increases. Also, it can be seen from the comparison between Figures 5, and 6 that the increase of Z softens the shell, which is in good agreement with the results of Dumir (1986 b).

Comparing Figures 2 to 4 and Figures 3 to 5, it can be noticed that the minimum value of the linear frequency corresponds to the maximum peak of the nonlinearity parameter. Also, the maximum value of the linear vibration frequency coincides with the minimum value of r.

The effect of the ratio γ on the nonlinearity parameter is plotted in Figure 7. For $2.5 < \gamma < 4$, the effect of geometric imperfection on the nonlinearity parameter is negligible, i.e; in this range, one may expect that the nonlinear vibration frequency is approximately the same as the linear one, at least for small values of vibration amplitude. In the presence of imperfection, the soft-spring behavior increases conceivably for $\gamma < 2.5$ and for $\gamma > 4$.

The effect of the circumeferential wave number n on the linear vibration frequency is reported in Figure 8 for perfect conical shell. The figure shows that for small value of γ , there is insignificant change in the linear vibration frequency as n increases. Meanwhile, as γ increases, the increase in the circumferential wave number is accompanied with a decrease in the linear vibration frequency.

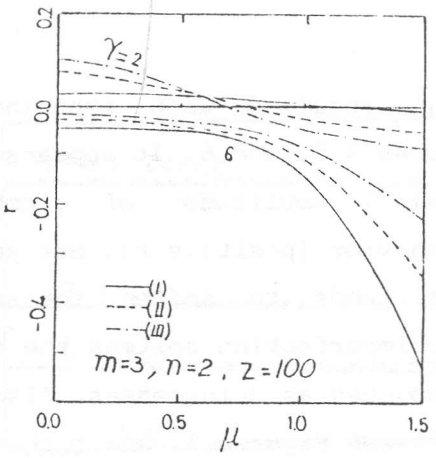

Figure 4: Nonlinearity parameter versus imperfection amplitude for m = 3, n = 2, Z = 100, γ = 2 and 6.

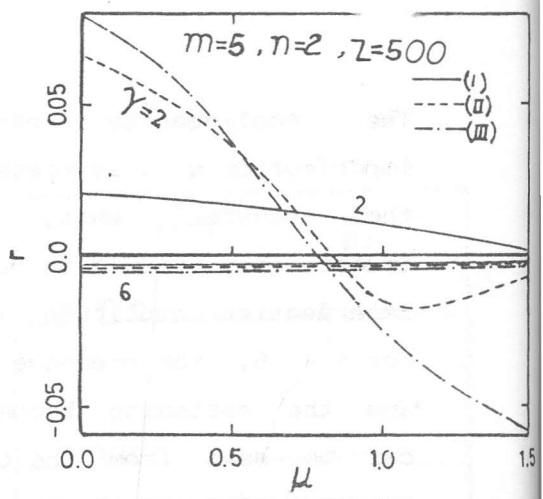

Figure 6: Nonlinearity parameter versus imperfection amplitude for m = 5, n = 2, Z = 500, γ= 2 and 6.

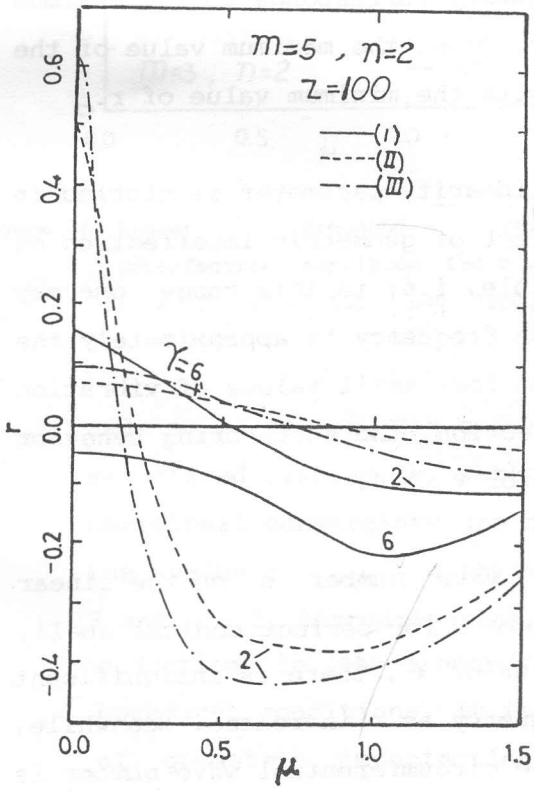

Figure 5: Nonlinearity parameter versus imperfection amplitude for m = 5, n = 2, Z = 100, γ= 2 and 6.

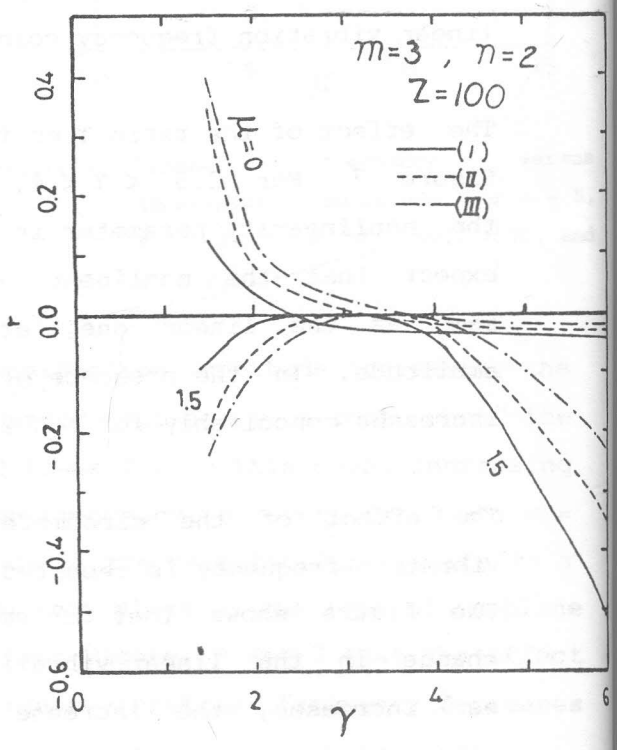

Figure 7: Nonlinearity parameter versus γ for m = 3, n = 2, Z = 100, μ =0 and 1.5.

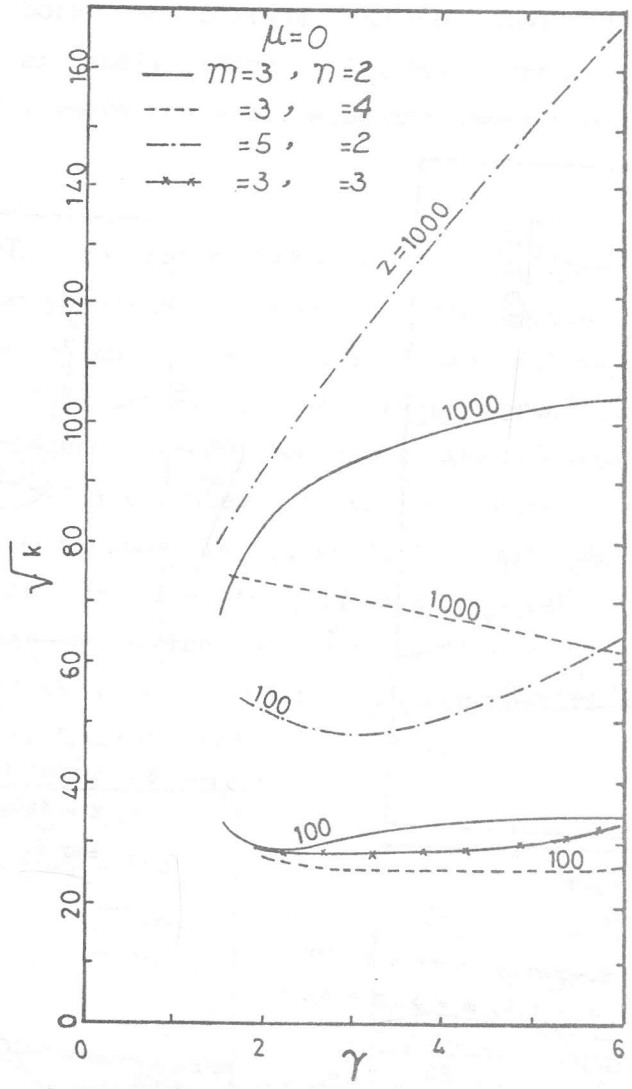

Figure 8: Linear frequency versus γ for perfect conical shell, Z = 100, 1000, m = 3,5, and n = 2,3, and 4.

However, in the presence of geometric imperfection (μ = 1.5), the increase in n results in an increase in the linear frequency especially for γ > 3 as shown in Figure 9. This is because the geometric imperfection is taken to be of the same shape as the

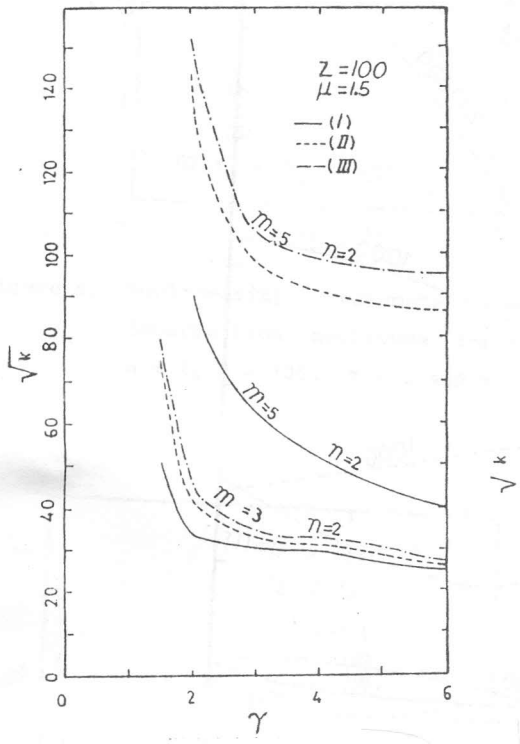

Figure 9: Linear frequency versus γ for Z = 100, μ = 1.5, m = 3, n = 2,3, and 4

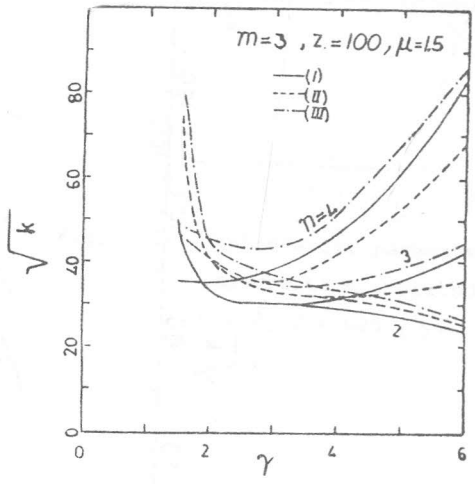

Figure 10: Linear frequency versus γ for Z = 100, μ = 1.5 , n = 2, m = 3, and 5.

vibration mode. One may also observe from Figure 9 that for n > 2, the linear vibration frequency for case II (no tangential constraints) are smaller than that in cases (I) and III where the tangential constraints are imposed. On the other hand, the increase in the meridional wave number m results in an increase in the linear

frequency for both the perfect conical shell (Figure 8) and the imperfect conical shell (Figure 10). The increase is pronounced for cases II and III where the shell ends are immovable in the meridional direction.

Figure 11 shows the ratio between the nonlinear to the linear vibration frequency versus the geometric imperfection for $\gamma = 2$, $Z = 100$, $m = 3$ and $n = 2$ for fixed values of the vibration amplitude $|X| = 0.5$ and 1.5. The increase in the amplitude of geometric imperfection tends to lower the nonlinear frequency for fixed X. This is attributed to the decrease of the nonlinearity parameter with μ as shown in Figure 4. For small values of geometric imperfection, the increase in $|X|$ raise the ratio Ω / Ω_o, while for large values of the nonlinear-to-linear, vibration frequency ratio is lowered as $|X|$ increases. Similar results are obtained for $m = 3$ and $n = 3$ as demonstrated in Figure 12.

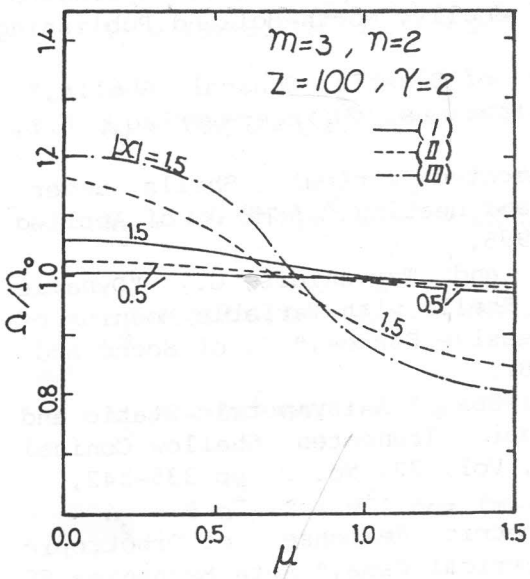

Figure 11: Nonlinear-to-linear frequency ratio versus imperfection amplitude for $Z = 100$, $\gamma = 2$, $m = 3$, $n = 2$, $|X| = 0.5$ and 1.5.

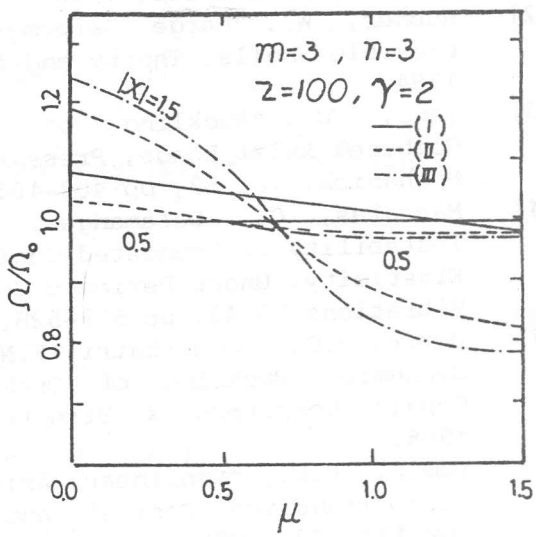

Figure 12: Nonlinear-to-linear frequency ratio versus imperfection amplitude for $Z = 100$, $\gamma = 2$, $m = 3$, $n = 3$, $|X| = 0.5$ and 1.5.

Conclusions

Effects of initial geometric imperfection, in-plane boundary conditions, and various geometric factors on large amplitude vibrations of truncated conical shell are investigated for $\beta = 30^{\circ}$. It was found that the linear vibration frequency for imperfect shell increases with the increase of the shape factor Z as well as the increase in the meridional wave number. But it decreases with the increase in the circumferential wave number. The presence of geometric imperfection softens the shell behavior instead of the hard-spring behavior of perfect conical shell. The softening increases as γ increases.

References

[1] Eslinger M., and Geier, R., "Buckling and Postbuckling Behavior of Conical Shell Subjected to Axisymmetric Loading and Cylinders Subjected to Bending," Theory of Shells, North-Holland Publishing Company, pp 263-288, 1980.

[2] Hubner, W., "Large Deformation of Elastic Conical Shells," Flexible Shells, Theory and Applications, Springer-Verlag, N.Y, 1984.

[3] Tani, J., "Buckling of Truncated conical Shells under Combined Axial Loads, Pressure, and Heating," ASME J. of Applied Mechanics, Vol 52, pp 402-408, 1985.

[4] Massalas, C., Dalamangas, A., and Tzrvanidis, G., "Dynamic Instability of Truncated Conical Shells with Variable Modulus of Elasticity, Under Periodic Compressive Forces," J. of Sound and Vibrations 79(4), pp 519-528, 1981.

[5] Dumir, P.C., and Khatri, K.N., 1986a, " Axisymmetric Static and Dynanmic Buckling of Orthotropic Truncated Shallow Conical Caps," Computers & Structures, Vol. 22, No. 3, pp 335-342, 1986.

[6] Dumir, P.C., "Nonlinear Axisymmetric Response of Orhotropic Thin Truncated Conical and Spherical Caps," Acta Mechanica 60, pp 121-132, 1986.

[7] Hui, D., "Large Amplitude Vibrations of Geometrically Imperfect Shallow Spherical Shells with Structural Damping," AIAA Journal, Vol. 21, No. 12, pp 1736-1741, 1983.

[8] Hui, D., "Effects of Geometric Imperfections on Large Amplitude Vibrations of Rectangular Plates with Hysteresis Damping," ASME Journal of Applied Mechanics, Vol. 51, pp 216-220, 1984.

[9] Hui, D., "Large Amplitude Axisymmetric Vibrations of Geometrically Imperfect Circular Plates,"J. of Sound and Vibration, Vol. 91, No. 2, pp 239-246, 1983.

[10] Hui, D. "In fluence of Geometric Imperfections and In-Plane Constraints on Nonlinear Vibrations of Simply Supported Cylindrical Pannels," ASME Journal of Applied Mechanics, Vol. 51, No.2, pp 383-390, 1984.

[11] Hui, D., and Du, I.H.Y., "Effects of Axial Imperfections on Vibrations of Anti-Symmetric Cross-Ply, Oval Cylinderical Shells," ASME Journal of Applied Mechanics, 86 - WAM, 1986.

[12] Watawala, L., and Nash, W.A., " Influence of Initial Geometric Imperfections on Vibrations of Thin Circular Cylindrical Shells, " Computers, Structures, Vol. 16, No. 1-4, pp 125-130, 1983.

Appendix

$$A_o = 12ZM[2(M^2-n^2)+(M^2+n^2)^2+1]/[M^2+n^2+1]^4$$

$$A_1 = (3/16)\,[M^2 + n^2 + 2n^2 \cos^2 (m+1)\pi\ n\ ]$$

$$A_2 = (3/16)\,[\ M^2 - 2M^2n^2 - n^2]/[M^2(M^2+1)]$$

$$A_3 = (3/16)\,[M^2 - n^2 - 2M^2n^2 - 2n^2 \cos^2(m+1)\pi\ n]/[n^2(1-n^2)]$$

$$A_4 = (3/16)(M^2 +n^2)/\ [M(M^2+1)]$$

$$A_5 = -\ 6n^2 \cos\ (m+1)\pi\ n\ /[M(4+M^2)^2]$$

$$A_6 = 6\ n^2\ (2 + M^2)\ \cos\ (m+1)\pi\ n\ /[M^2(4+M^2)]$$

$$A_7 = (3/16\ B_1)\ [\ M^2(1+M^2-n^2)\ -\ M^2n^2\ (1+M^2+n^2)$$

$$-\ n^2\ (M^2 + 2M - 1)\ (\ 1-\ M^2\ -\ n^2)\ ]$$

$$A_8 = (3/16\ B_1)\ [\ M^5 + M^3 - 4M^2n^2 + 3Mn^2 - Mn^4]$$

$$A_9 = (3/64B_2)[2M^2n^2(M^2+4n^2)-4n^2(4+3M^2-4n^2)]\ [\cos\ (m+1)\pi\ \ n\ ]$$

$$A_{10} = -\ (3/64\ B_2)\ [2\ Mn^2(4+5M^2+4n^2)]\ \cos\ (m+1)\pi\ n$$

where

$$B_1 = [M^2 + n^2][(1+M^2-n^2)^2 + 4M^2n^2]$$

$$B_2 = [M^2/4 + n^2][(1+M^2/4 - n^2)^2 + M^2n^2]$$

Case I

$$E_1 = (9n^2/8)[1+2\ \cos^2(m+1)\pi\ n\ ] - 3M^2/8$$

$$E_2 = (3/4)\ [n^2 - M^2 + 2n^2\ \cos\ (m+1)\pi\ n\ ]$$

Case II

$$E_1 = -\ (3/8)\ [M^2 + n^2 + 2n^2\ \cos^2\ (m+1)\pi\ n\ ]$$

$$E_2 = (3/4)\ [M^2 - n^2 - 2n^2\ \cos\ (m+1)\ \pi\ n]$$

Case III

$$E_1 = (3/2)\ [n^2 + 2n^2\ \cos^2\ (m+1)\pi\ n + \nu M^2]/(1-\ \nu^2) - 2A_1$$

$$E_2 = (3/2)\ [M^2 + \nu n^2 + 2\nu n^2\ \cos^2\ (m+1)\pi\ n]/(1-\ \nu^2) + E_1 - 2A$$